Size-dependent tunneling differential conductance spectra of crystalline Pd nanoparticles

Bing Wang, Kedong Wang, Wei Lu, Jinlong Yang, and J. G. Hou*
Hefei National Laboratory for Physical Sciences at Microscale, Structure Research Laboratory, University of Science and Technology of China, Hefei, Anhui 23026, China

(Received 29 April 2004; revised manuscript received 29 July 2004; published 11 November 2004)

The single-electron tunneling behavior of crystalline palladium nanoparticles with narrowly distributed core sizes ranging from 1.6 to 4 nm is studied by scanning tunneling microscopy/spectroscopy. The current-voltage (*I-V*) characteristics of Pd nanoparticles exhibit size-dependent fine features, which are assigned to the discreteness of energy states of the ultrasmall Pd particles. It is found that the peak widths, as well as the intrapeak spacings in differential conductance dI/dV spectra increase with the decrease of the size of Pd nanoparticles. Our analysis shows that the dwell time of the weak tunnel junction may not be a major contribution to the peak widths due to the large resistance of the tunnel junction of about $10^7\Omega$. The possible effect of residual charge is also excluded. An explanation of the size-dependent behaviors of the peak width and the intrapeak spacing is attributed to the clustered electronic structures around the Fermi level due to certain size-dependent dynamic effects.

DOI: 10.1103/PhysRevB.70.205411 PACS number(s): 73.22.−f, 68.37.Ef, 73.23.Hk

I. INTRODUCTION

In ultrasmall metallic grains, dynamic effects play important roles to their electronic structures, and thus affect the electron transoport.[1–4] Single-electron tunneling spectroscopy has been used to probe the dynamic effects of metallic nanoparticles in the characteristics of the discrete states in conductance spectra.[1,2,5] It provides a direct method to study the individual energy levels of semiconductor quantum dots (QDs) in the case that the single-electron charging energy, E_c, is on the order of or smaller than the typical discrete energy-level spacings, δE, due to their relatively low densities of states.[6–14] Using the method, the atomiclike shell structures of QDs were revealed.[8,10–12] In the tunneling conductance spectra, dI/dV-V, the peaks exhibited a systematic broadening with the reduction of dot diameter, which was assigned to a decreased electron dwell time on the dot due to the size dependent barrier height.[12] However, unlike the semiconductor QDs, the charging energy of a metal particle in nanometer scale is typically much larger than the discrete energy level spacings. In this case, the measured discrete states contain contributions from many-electron excitations,[4,15,16] and therefore, it may not be simply understood as the independent-electron picture as in semiconductor QDs. Moreover, the behaviors of the peak widths and the intrapeak spacings in the tunneling conductance spectra for metal particles are not adequately studied and less understood.

The observation of discrete energy levels of metal nanoparticles were reported mostly at dilution refrigerator temperatures using fabricated devices in which a metal particle coupled two electrodes to form a double barrier tunneling junction.[15–23] Very recently, discrete energy levels of ultrasmall metal nanoparticles have also been observed by scanning tunneling microscopy/spectroscopy (STM/STS) at temperature of 5 K.[5,24–27] This profits from the synthesis of ultrasmall ligand-stabilized, narrow size distributed metal nanoparticles via the wet-chemical method.[28–32] The core sizes of the metal particles are identified by high resolution electron microscopy (HREM). Hence, it is possible to systematically investigate the size-dependent properties of the metal particles with well-defined sizes. Both E_c and δE are particle size dependent, which can be reflected in the current-voltage (*I-V*) curves of single-electron tunneling. Moreover, due to the size-dependent dynamic effects,[33,34] the electron-electron scattering lifetime will be size dependent, and hence reflected in the *I-V* characteristics. Thus, it is interesting to study the size-dependent tunneling behaviors of metal nanoparticles.

In this paper, we present a systematic analysis of the tunneling spectra of crystalline palladium nanoparticles with size ranging from 1.6 nm to 4 nm in diameter. The peak width and the effect of discrete energy levels have been compared with the simulated results based on orthodox theory for single-electron tunneling.[35,36]

II. EXPERIMENT

The crystalline Pd particles used in our experiment were synthesized using chemical method which produced nearly monodispersed ultrasmall crystalline Pd nanopartciles.[29] Pd particles were refined by fractionation, and particles with narrow distributed sizes of 1.6 nm, 2 nm, 2.2 nm, 2.5 nm, 3 nm, and 4 nm in diameter were measured with STM/STS. The samples were prepared by spreading drops of the toluene solutions containing the Pd crystalline nanoparticles on several pieces of freshly grown Au (111) films (160 nm thick) on mica. The samples on Au/mica substrates were introduced into the cryostat of Omicron's ultrahigh vacuum low temperature scanning tunneling microscope, which was precooled down to 5 K. Before measuring, we waited about 2 h for stabilization of the tip of the microscope and the sample. The drift between the tip and the sample could be as small as 0.1 nm/h. A typical voltage sweeping period for a single *I-V* curve with about 2000 points was about 3 s.

The *I-V* curves of individual Pd particles with determined sizes were measured by positioning the tip of the microscope over a selected Pd nanoparticle while turning off the feedback of the microscope. Here, the tip of the microscope, the

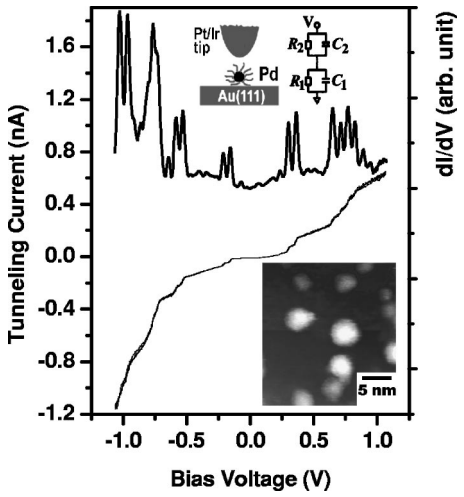

FIG. 1. Four representative *I-V* curves taken at a set point of 1.8 V and 1.0 nA in successive four repeats and one of the numerical dI/dV spectra for a Pd nanoparticle of 2 nm in diameter. The four *I-V* curves nearly thoroughly overlap. The upper inset is a schematic of the STM double barrier tunnel junction, and the lower inset shows an STM image of the particles with average core size of 2 nm in diameter.

thiol-capped Pd nanoparticle, and the Au substrate formed a double barrier tunneling junction (DBTJ),[5,25] as depicted in the upper inset in Fig. 1. An STM image of Pd nanoparticles with average core size of 2 nm in diameter (characterized by HREM) is shown in the lower inset in Fig. 1, where the particle sizes in the STM image are larger than the averaged core size due to the effect of the tip convolution and the capped thiols. The electrochemically etched Pt/Ir tip was carefully treated and cleaned in vacuum before it was used.

III. RESULTS AND DISCUSSION

Representative *I-V* curves and one of the numerical differential dI/dV for a crystalline Pd particle of 2 nm in diameter are shown in Fig. 1. The *I-V* curves (in lower panel), which are taken at the same set-point of 1.8 V and 1.0 nA in successive four repeats, nearly thoroughly overlap, indicating the high reproducibility of the *I-V* curves. There are fine features in addition to the main steps. The main current steps are due to the single-electron charging effect, while the fine features are attributed to the effect of the discreteness of energy states of ultrasmall crystalline Pd nanoparticles due to the multichannels of discrete states.[1,5,24,37] The fine features can be seen much clearly as the multipeaks in the dI/dV curve (in upper panel). There was a quite asymmetric junction configuration in our experiment, hence, the multipeaks in a dI/dV curve may reflect the structure of the particle energy spectrum.[10,12] Here, the behavior of the fine peaks is different from the case of semiconductor QDs.[10,12] In the case of the semiconductor QDs, since the level spacings are much larger than the charging energy, $\delta E > E_c$, the single-electron tunneling happens via degenerated discrete levels, thus two and up to sixfold charging multiplets in tunneling spectra reflect the spherical atomiclike QD states with *s* and *p* symmetries. The separation within the multiplets is determined by the single-electron charging energy, and the separation between two groups of peaks is a sum of the level spacing δE and the charging energy E_c. Whereas, $\delta E \ll E_c$ in Pd nanoparticles of around 2 nm in diameter, typically, the magnitude for δE is in range of about 20–60 meV, and $E_c > 100$ meV.[5,24,25] Though the measured intrapeak spacings of the multipeaks are qualitatively in agreement with the expected spacings of the energy levels, the further analysis shows that each of the peaks, unlike the case of the semiconductor QDs, may not directly reflect the single states, but, as we will show below, the clumping of states caused by complicated dynamic effects.

In the case of the metal nanoparticles, much higher voltage (or energy) resolutions of conductance spectra have been obtained under dilution refrigerator temperatures using tunneling devices by several groups.[15–23] Ralph *et al.*[15,18,21] observed the discrete electronic states in the conductance spectra for aluminum nanoparticles. Their results show that for larger particles the fine substructures in the conductance spectra exhibit single peaks, which reflect the discrete energy levels.[21] The peak spacings are in agreement with the estimated mean level spacing. However, for smaller particles, the energy resonances at low energies are grouped in clusters spaced in the order of the mean level spacing, and the first cluster contains only one peak, but the resonances at higher energies consist of much closer spaced clusters than the mean level spacing. To understand the clustered structure, Agam *et al.* presented a picture that each cluster of resonances is identified nonequilibrium occupancy configurations of the other single-electron states.[19] This analysis is based on the condition that the rate Γ^{inel} of inelastic relaxation processes is smaller than the tunneling rate of an electron into and out of the dot, Γ^{tun}. When $\Gamma^{\text{inel}} > \Gamma^{\text{tun}}$, the system relaxes to equilibrium between tunneling events, then each resonance cluster collapses to a single peak, as the case for the larger Al particles in the observations by Ralph *et al.*. A similar behavior has been observed in Au nanoparticles by Davidović and Tinkham.[16] These measurements were mainly concentrated around the first Coulomb blockade step, i.e., there was only one extra electron tunneling into or out of the dots $(n_0 \pm 1)$, while our measurements extended to higher progressions of steps, which have more than one electron into or out of the dots. The fine features around the main steps (Fig. 1) resemble the previous observations of discrete energy states in metal particles, but may not give the detailed information for each state as those due to a lower voltage resolution.

It is noted that there is an increasing peak width, as well as the increasing separation between multipeaks in the conductance spectra as the particle size reduces, as shown in Fig. 2. For a larger crystalline particle (say, the curve for Pd of 3 nm and 4 nm in diameter), the peak splits can be just recognized around the main peaks. When the particle size is smaller than 2.5 nm, the multipeaks are well separated, though the widths of multipeaks broaden with the decrease of the particle size. Here, we need to exclude any possible effects from the tunneling barriers and the residual charging. In our measurements, the weak tunnel junction is generally the substrate-particle junction, while the tip-particle junction

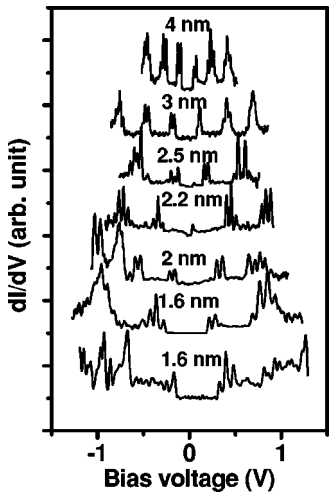

FIG. 2. Conductance spectra features of crystalline Pd particles with diameter in ranging of 1.6–4 nm. For clarity, curves shift vertically.

has much larger resistance than the substrate-particle junction due to the existing vacuum gap between the tip and the particle. By synthesis of Pd particles of 2 nm in diameter coated using different alkanethiols of decanethiol (C_{10}), dodecanethiol (C_{12}), and hexadecanethiol (C_{16}), we changed the resistance of the substrate-particle junction, but we did not observe obvious change in the peak widths and the intrapeak spacings, as shown in Fig. 3(a). Though the gaps of the substrate-particle junctions may not linearly correspond to the chain lengths of the ligands due to the deformation of the alkyl chain, it at least shows that the peak widths and the intrapeak spacings are not sensitive to the resistance of the weak junction in our case. As a further test, we changed the gap of the tip-particle junction by adjusting the set-point current of the microscope. A series of dI/dV curves with different gaps of the tip-particle junction is plotted in Fig. 3(b). The peak widths and the intrapeak spacings of the fine peaks are observed without obvious change, though the positions of the peaks shift due to a possible change in the residual charge, Q_0.[35,36] It was observed that even Q_0 varied in a relatively wide range, both the peak widths and the intrapeak spacings change little. Moreover, as shown in Fig. 3(c1)–(c3), when Q_0 varies from 0.08e to 0.48e, where e is the electron charge, one can see that while the fine features in I-V curves (or the peaks in dI/dV curves) shift with the change of Q_0 and the zero conductance region changes from about 210 meV to nearly total suppression, the peak widths and the intrapeak spacings in dI/dV curves nearly remain unchanged. As shown in Fig. 1, all of the I-V curves are highly reproducible for the same particle with the same set-point conditions. Here, we further show that the reproducibility is independent on the voltage sweeping speed. Several sets of two I-V curves measured with voltage sweeping periods of 1.5 s and 3 s are plotted in Fig. 3(c). The two I-V curves for each set give nearly the same features even with different voltage sweeping speeds. However, there are some differences in conductance spectra for different particles with a similar size. As shown in Fig. 2 for the two curves labeled 1.6 nm, they were obtained from different particles with a similar size of 1.6 nm. Though the main features of multipeaks are similar, the detailed structures are different, which may reflect the differences in the electronic structures resulting from the possible variations in the atomic structures for different particles. We believe that, unlike the case of semiconductor QDs, the major contribution to the peak width in the case of the Pd particles may not be assigned to the dwell time of the junction, and the possible contribution from residual charge can be excluded, other than, the size-dependent peak widths and the intrapeak spacings may reflect the electronic structures of Pd particles, and possibly the electron-electron interaction of the nanoparticle.[5]

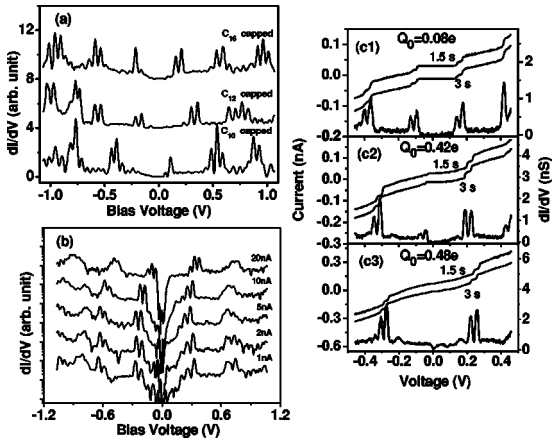

FIG. 3. (a) Conductance spectra for the Pd particles capped with alkanethiols of C_{10}, C_{12}, and C_{16}. (b) Conductance spectra for a Pd particle of about 2 nm in diameter with different set-point currents. (c) Sets of two I-V curves measured with voltage sweeping periods of 1.5 and 3 s, for different residual charging conditions, (c1) 0.08e, (c2) 0.42e, and (c3) 0.48e. Numerically differentiated dI/dV spectra corresponding to the I-V curves measured with a sweeping period of 3 s are plotted. For clarity, curves are shifted vertically.

In our observations, the peak widths are much large, even up to 40 meV, which may not directly reflect the homogenous linewidth of energy levels. It is also necessary to further analyze the size-dependent behaviors of the peak widths and the intrapeak spacings. To show the size-dependent behaviors clearly, we plot the full width at half-maximum (FWHM), Δ, and the intrapeak spacings of the multipeaks, δ, against the charging energy E_c in Fig. 4(a). We estimated the charging energy by $E_c = e^2/2(C_1+C_2)$, where C_1 and C_2 were obtained from the fit of the I-V curves using orthodox theory[35,36] by just considering the position of the main steps.[5] The peak widths were obtained by a fit using Lorentzian line shape. The error bars show the fluctuation in the charging energy, the peak spacings, and the peak widths correspondingly. The particle sizes in top axis in Fig. 4(a) are estimated from the HREM images. Such a behavior of the size-dependent peak widths is similar to that for the semiconductor QDs.[12] Millo *et al.* attributed the size dependent broadening to the dwell time via the weak tunnel junction resulting from the confinement effect. In their case, a quite small resistance of $\sim 10^5\Omega$ was derived for the weak tunnel junction. However, a much larger resistance of $\sim 10^7\Omega$ was obtained in our STM configuration[5,24,25] using a least square fit by orthodox theory.[35,36] Such a resistance corresponds to a quite

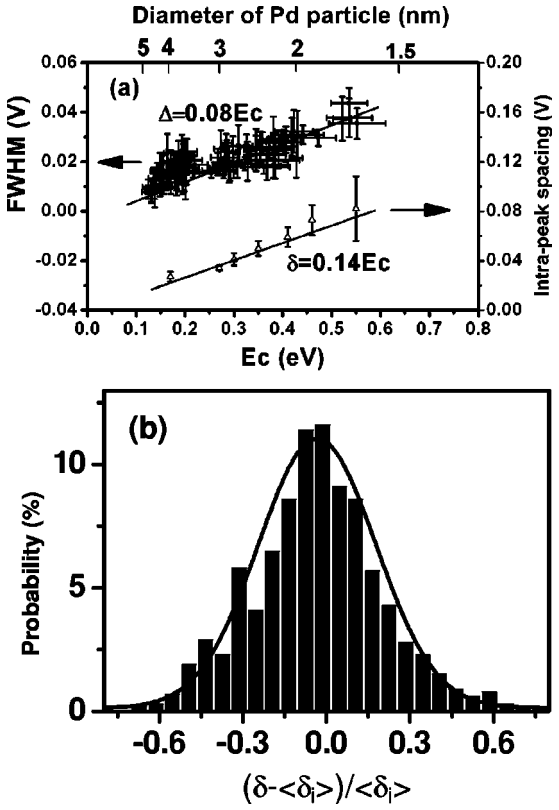

FIG. 4. (a) Statistics of the peak widths and the intrapeak spacing in conductance spectra against charging energy E_c. (b) Histogram of the normalized fluctuation in the intrapeak spacings, along with a fit to a Gaussian distribution (solid line).

small contribution of less than 1 meV to the peak widths estimated from the uncertainty relation. Even considering the thermal broadening of about 1 meV ($3.5k_BT$, where k_B is Boltzmann's constant, and T is temperature) and the experimental resolution of about 2 mV, we still have quite a large difference between the estimated values of the peak widths and the experimental ones.

One may note that in Fig. 4(a), both the peak width and the intrapeak spacing of the fine peaks nearly linearly increase with the increasing of the separation of the Coulomb charging peaks. The linear fit gives $\Delta=(0.08\pm0.01)E_c$ and $\delta=(0.14\pm0.03)E_c$ [as the solid lines shown in Fig. 4(a)] using the form $\Delta_i=b_0+b_1E_c$ (Δ_i denotes Δ and δ, respectively), where $b_0\simeq0$ are obtained for both of the fits. The distribution of the intrapeak spacings is plotted as histogram in Fig. 4(b), which is normalized followed by a similar procedure as in Refs. 12, 38, and 39. The distribution is found to be Gaussian other than the description of random matrix theory, different from the calculation by Narvaez and Kirczenow.[40] Such a "universal behavior of Gaussian" reflects a strong Coulomb interaction rather than single particle level fluctuations. Here, the fluctuation in intrapeak spacings increases with the decreasing of the particle sizes, which may reflect a much wider variation in differences of eigenenergies of eigenstates around the Fermi level in smaller particles than in larger ones in the electronic structures. This is coincident to our results for crystalline Pd using the tight-binding method,[5,24] and to the calculation for Al nanoparticles coated with Al oxide,[40] where for small particles the large surface to volume ratios should have a significant effect on the level spacings.

To understand the experimental results shown above, one may need to consider the electronic structures of crystalline Pd nanoparticles. Metals have very high densities of states, hence, a metal particle has relatively small discrete energy level spacings, e.g., $\delta E\ll E_c$. In most of the discussions, the level spacings were treated as the independent-electron particle-in-a-box spacings. The single-particle discrete states are expected to be resolvable when several conditions are met:[1] (1) $k_BT\ll\delta E$; (2) $\hbar\Gamma^{\mathrm{tun}}\ll\delta E$, where Γ^{tun} is the tunneling rate out of a discrete state on the metal particle into a coupled lead (here is the tip or the substrate); (3) $\hbar\Gamma^{\mathrm{inel}}<\delta E$, where Γ^{inel} is the inelastic relaxation rate of the excited state on the nanoparticle with an energy ϵ above the ground state, which can be met when $\epsilon<E_{\mathrm{Th}}$, where the Thouless energy E_{Th} is the inverse time for an electron near the Fermi level to travel across the nanoparticle.[4] As discussed above, the first two conditions are met in our measurement. Here, we need to consider the third condition, which depends on the dimensionless conductance $g=E_{\mathrm{Th}}/\overline{\delta E}$, where $\overline{\delta E}$ is the average independent-electron particle-in-a-box spacings estimated by $\overline{\delta E}\sim2\pi^2\hbar^2/mk_F\mathcal{V}$. Here, $\mathcal{V}$ is the volume of the particle, m is the electron mass, and k_F is the Fermi wave vector, about 12.6 nm^{-1} for Pd. One conduction electron for a Pd atom is assumed. For a ballistic limit, where the Thouless energy E_{Th} is estimated by $E_{\mathrm{Th}}\sim\hbar v_F/aD$ (Fermi wave velocity $v_F\sim1.5\times10^8$ cm/s for Pd, and $a=3$), we obtain $g\sim5$ and $E_{\mathrm{Th}}\sim140$ meV for Pd nanoparticle with the diameter of $D=2$ nm. The criterion $\epsilon^*=\overline{\delta E}\sqrt{g}\sim66$ meV. When $\epsilon>\epsilon^*$, golden rule is applicable, and hence, the orthodox theory can be used to describe the tunneling behavior via discrete states.[4]

In previous investigations on metal nanoparticles, the concentration is almost focused on the fine features of the voltage range just beyond the Coulomb-blockade threshold at very low temperature of sub-Kelvin, due to the relatively large particles involved. In these cases, even the many-electron states may be coupled in, the quasiparticle states can still be resolved at energy range of $\epsilon^*<\epsilon<E_{\mathrm{Th}}$. Whereas, for much smaller metal particles, due to the complexity of the processes involved, such as enhanced electron-electron and electron-phonon interactions,[5,33,34] and many-body interactions,[4] the complete understanding is not currently available. Though we attribute the observed fine features in I-V curves or dI/dV spectra to the discreteness of the electronic structures for such ultrasmall nanoparticles at elevated temperature of 5 K, we still lack the detailed knowledge about them. The highest energy at which the quasiparticle can be resolved is predicted to be the Thouless energy.[3] However, as pointed out by Ralph *et al.*[15] and Altschuler *et al.*,[4] the many-electron interaction should be taken into account. In such a case, the single-electron particle-in-a-box eigenstates associated with many-electron states lead to clumping of states, and the density of accessible many-electron eigenstates should be expected to grow with increasing electron energy, quickly becoming greater than the single-electron estimate when $\epsilon>\epsilon^*$. Our measurements for the Pd particle size ranging from 1.6–4 nm fall in the regime.

Moreover, the relaxation process may be important in determination of the fine features in the conductance spectra. According to the model by Agam *et al.*,[19] we may identify that the system is in the equilibrium regime or in the nonequilibrium regime. In our STM configuration, the junction resistance is in the order of $10^7\Omega$, corresponding to a tunneling rate Γ^{tun} of about 10^{11} s^{-1} considering a voltage drop of 0.2 V in the junction. The rate Γ^{inel} of inelastic relaxation processes is estimated by taking the electron-electron scattering and electron-phonon scattering into account,[5] and obtained in the order of 6×10^{12} s^{-1}. Since $\Gamma^{\text{inel}}>\Gamma^{\text{tun}}$, the system is far from nonequilibrium but in the equilibrium regime. Hence, the fine features of the multipeaks in conductance spectra behave like the observations by Ralph *et al.* for the larger Al particles of 130 nm^3 in volume.[15,21] However, due to lower voltage resolution than the observations by Ralph *et al.*, the single states are not resolved in our results, instead, each peak in conductance spectra may contain the contribution of level clusters. We noted that in the results by Ralph *et al.*,[21] though the spacings between the single peaks in principle are in agreement with the mean level spacing, the single peaks are not equally spaced. Such a nonequidistant behavior in electronic structure may become significant in a much smaller particle, say, 2 nm in diameter or 4.2 nm^3 in volume of a Pd sphere. And more important the many-body effects may be enhanced in such an ultrasmall particle. Thus, the clustered electronic states form, and may be reflected with a few peaks in conductance spectra by smearing small spaced states due to certain convolution effects.

Based on the observations and the discussions above, it is possible to simulate the experimental results phenomenologically. From our calculation of Pd nanoparticles based on the tight-binding method, the energy levels are clustered in groups,[5,24] which is in agreement to the calculation for Al nanoparticles coated with Al oxide with a similar method.[40] But, such a calculation is insufficient to understand the size-dependent behaviors shown above. Considering that for the Pd nanoparticles in the range of 1.6–4 nm, $E_c\propto D^{-1}$ from Fig. 4(a), then, we have $\Delta\propto D^{-1}$, and $\delta\propto D^{-1}$. As indicated by Sivan *et al.*, only in the range of Thouless energy around Fermi level the energy levels are discrete, while they become continuous in energy farther than the Thouless energy from the Fermi level due to the interaction beyond the average level spacing.[3] For simplicity, we assume several discrete states, which contain size-dependent clustered groups, around the Fermi level similar to the case in Ref. 3, as shown in Fig. 5(a), then, we may qualitatively simulate the experimental results using orthodox theory,[35,36] as shown in Fig. 5(b). In Fig. 5(b), we observed that the peak widths and the intrapeak spacings of the multipeaks in the conductance spectra nearly directly correspond to the widths and the spacings of the assumed electronic structures, respectively. One may note that the simulation gives nearly the same structure around the different main peaks, which is different from the experimental observations. This is because the model for simulation did not consider the effects of different numbers of extra electrons on the particles and the energy dependent effects. The electron interactions, maybe important for the ultrasmall particles, may be different when the number of the extra electrons into or out of the particle is more than one,

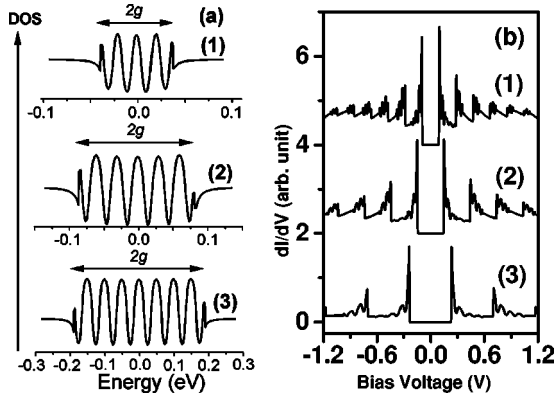

FIG. 5. (a) Assumed electronic structures with discrete clustered energy states: (1) spacing 20 meV, width 10 meV, (2) spacing 30 meV, width 20 meV, and (3) spacing 50 meV, width 30 meV. (b) Corresponding simulated dI/dV spectra using the assumed electronic structures in (a) by the orthodox theory with parameters of (1) $C_1=0.30$ aF, $C_2=0.80$ aF, (2) $C_1=0.30$ aF, $C_2=0.54$ aF, (3) $C_1=0.30$ aF, $C_2=0.34$ aF, respectively, while keeping $R_2/R_1=5$, $R_1=80$ MΩ, residual charge $Q_0=0$, and $T=4.2$ K.

which results in the different behaviors around the main steps. Though the model for the simulation is simple, the results show that the size-dependent clustered electronic structures may be the possible reason that causes the size-dependent peak widths and the size-dependent peak spacings in single-electron tunneling spectra.

IV. CONCLUSIONS

We have studied the size-dependent behavior of the peak widths of dI/dV in single-electron tunneling spectra by STM/STS at 5 K. Crystalline Pd nanoparticles with narrow size distribution ranging 1.6 to 4 nm were synthesized. Fine peaks were observed in dI/dV spectra in addition to the Coulomb blockade and Coulomb staircases, which are attributed to the discreteness of energy levels. The peak widths and the intrapeak spacings were size dependent. Our analysis shows that the possible effects of tunnel junction and residual charge on the peak widths and the intrapeak spacings can be excluded. The fine peaks may not directly reflect the single discrete states, but clustered groups of levels caused by certain dynamic effects. The phenomenological simulation by assuming size-dependent clustered electronic structures around the Fermi level qualitatively accords with the experimental observation, and thus, we attribute the size-dependent behaviors of the peak widths and the intrapeak spacings to the clustered electronic structures of ultrasmall Pd nanoparticles due to size-dependent dynamic effects.

ACKNOWLEDGMENTS

This work was supported by the National Project for the Development of Key Fundamental Sciences in China (Grant No. G2001CB3095), by the National Natural Science Foundation of China (Grant Nos. 50121202, 50132030, 10374083).

*Electronic address: jghou@ustc.edu.cn

[1] For a review, see J. von Delft and D. C. Ralph, Phys. Rep. **345**, 62 (2001).
[2] U. Sivan, F. P. Milliken, K. Milkove, S. Rishton, Y. Lee, J. M. Hong, V. Boegli, D. Kern, and M. deFranza, Europhys. Lett. **25**, 605 (1994).
[3] U. Sivan, Y. Imry, and A. G. Aronov, Europhys. Lett. **28**, 115 (1994).
[4] B. L. Altshuler, Y. Gefen, A. Kamenev, and L. S. Levitov, Phys. Rev. Lett. **78**, 2803 (1997).
[5] J. G. Hou, B. Wang, J. L. Yang, K. D. Wang, W. Lu, Z. Y. Li, H. Q. Wang, D. M. Chen, and Q. S. Zhu, Phys. Rev. Lett. **90**, 246803 (2003).
[6] Y. Alhassid, Rev. Mod. Phys. **72**, 895 (2000).
[7] D. M. Mittleman *et al.*, Phys. Rev. B **49**, 14 435 (1994).
[8] L. P. Kouwenhoven, T. H. Oosterkamp, M. W. S. Danoesastro, M. Eto, D. G. Austing, T. Honda, and S. Tarucha, Science **278**, 1788 (1997).
[9] D. R. Stewart, D. Sprinzak, C. M. Marcus, C. I. Duruoz, and J. S. Harris, Jr., Science **278**, 1784 (1997).
[10] U. Banin, Y. W. Cao, D. Katz, and O. Millo, Nature (London) **400**, 542 (1999).
[11] O. Millo, D. Katz, Y. W. Cao, and U. Banin, Phys. Rev. Lett. **86**, 5751 (2001).
[12] O. Millo, D. Katz, Y. W. Cao, and U. Banin, Phys. Rev. B **61**, 16 773 (2000).
[13] B. Alperson, S. Cohen, I. Rubinstein, and G. Hodes, Phys. Rev. B **52**, R17 017 (1995).
[14] B. Alperson, I. Rubinstein, G. Hodes, D. Porath, and O. Millo, Appl. Phys. Lett. **75**, 1751 (1999).
[15] D. C. Ralph, C. T. Black, and M. Tinkham, Physica B **218**, 258 (1996).
[16] D. Davidović and M. Tinkham, Phys. Rev. Lett. **83**, 1644 (1999).
[17] C. T. Black, D. C. Ralph, and M. Tinkham, Phys. Rev. Lett. **76**, 688 (1996).
[18] D. C. Ralph, C. T. Black, and M. Tinkham, Phys. Rev. Lett. **78**, 4087 (1997).
[19] O. Agam, N. S. Wingreen, B. L. Altshuler, D. C. Ralph, and M. Tinkham, Phys. Rev. Lett. **78**, 1956 (1997).
[20] O. Agam and I. L. Aleiner, Phys. Rev. B **56**, R5759 (1997).
[21] D. C. Ralph, C. T. Black, and M. Tinkham, Phys. Rev. Lett. **74**, 3241 (1995).
[22] S. Guéron, M. M. Deshmukh, E. B. Myers, and D. C. Ralph, Phys. Rev. Lett. **83**, 4148 (1999).
[23] D. G. Salinas, S. Guéron, D. C. Ralph, C. T. Black, and M. Tinkham, Phys. Rev. B **60**, 6137 (1999).
[24] B. Wang, K. D. Wang, W. Lu, H. Q. Wang, Z. Y. Li, J. L. Yang, and J. G. Hou, Appl. Phys. Lett. **82**, 3767 (2003).
[25] B. Wang, H. Q. Wang, H. X. Li, C. G. Zeng, J. G. Hou, and X. D. Xiao, Phys. Rev. B **63**, 035403 (2001).
[26] J. G. A. Dubois, J. W. Gerritsen, S. E. Shafranjuk, E. J. G. Boon, G. Schmid, and H. van Kempen, Europhys. Lett. **33**, 279 (1995).
[27] H. Zhang, G. Schmid, and U. Hartmann, Nano Lett. **3**, 305 (2003).
[28] M. Brust, M. Walker, D. Bethell, D. J. Schiffrin, and R. Whyman, J. Chem. Soc., Chem. Commun. **1994**, 801 (1994).
[29] W. Lu, B. Wang, K. Wang, X. Wang, and J. G. Hou, Langmuir **19**, 5887 (2003).
[30] R. L. Whetten, J. T. Khoury, M. M. Alvarez, S. Murthy, I. Vezmar, Z. L. Wang, P. W. Stephens, C. L. Cleveland, W. D. Luedtke, and U. Landman, Adv. Mater. (Weinheim, Ger.) **8**, 428 (1996).
[31] M. J. Hostetler, J. E. Wingate, C. J. Zhong, J. E. Harris, R. W. Vachet, M. R. Clark, J. D. Londono, S. J. Green, J. J. Stokes, G. D. Wignall, G. L. Glish, M. D. Porter, N. D. Evans, and R. W. Murray, Langmuir **14**, 17 (1998).
[32] H.-G. Boyen, G. Kästle, F. Weigl, P. Ziemann, G. Schmid, M. G. Garnier, and P. Oelhafen, Phys. Rev. Lett. **87**, 276401 (2001), and references therein.
[33] N. Pontius, G. Lüttgens, P. S. Bechthold, M. Neeb, and W. Eberhardt, J. Chem. Phys. **115**, 10479 (2001).
[34] C. Voisin *et al.*, Phys. Rev. Lett. **85**, 2200 (2000).
[35] A. E. Hanna and M. Tinkham, Phys. Rev. B **44**, 5919 (1991).
[36] M. Amman, R. Wilkins, E. Ben-Jacob, P. D. Maker, and R. C. Jaklevic, Phys. Rev. B **43**, 1146 (1991).
[37] D. V. Averin and A. N. Korotkov, J. Low Temp. Phys. **80**, 173 (1990); D. V. Averin, A. N. Korotkov, and K. K. Likharev, Phys. Rev. B **44**, 6199 (1991).
[38] U. Sivan, R. Berkovits, Y. Aloni, O. Prus, A. Auerbach, and G. Ben-Yoseph, Phys. Rev. Lett. **77**, 1123 (1996).
[39] R. Berkovits, Phys. Rev. Lett. **81**, 2128 (1998).
[40] G. A. Narvaez and G. Kirczenow, Phys. Rev. B **65**, 121403 (2002).